

Rapid concentration and elution of malarial antigen histidine-rich protein II using solid phase Zn(II) resin in a simple flow-through pipette tip format

Westley S. Bauer,^{1,a)} Kelly A. Richardson,^{1,a)} Nicholas M. Adams,²
 Keersten M. Ricks,¹ David J. Gasperino,³ Simon J. Ghionea,³
 Mathew Rosen,³ Kevin P. Nichols,³ Bernhard H. Weigl,³
 Frederick R. Haselton,^{1,2} and David W. Wright¹

¹Department of Chemistry, Vanderbilt University, Nashville, Tennessee 37235, USA

²Department of Biomedical Engineering, Vanderbilt University, Nashville, Tennessee 37235, USA

³Intellectual Ventures Laboratory, 14360 SE Eastgate Way, Bellevue, Washington 98007, USA

(Received 5 April 2017; accepted 18 May 2017; published online 2 June 2017)

Rapid diagnostic tests (RDTs) designed to function at the point of care are becoming more prevalent in malaria diagnostics because of their low cost and simplicity. While many of these tests function effectively with high parasite density samples, their poor sensitivity can often lead to misdiagnosis when parasitemia falls below 100 parasites/ μl . In this study, a flow-through pipette-based column was explored as a cost-effective means to capture and elute more *Plasmodium falciparum* histidine-rich protein II (HRPII) antigen, concentrating the biomarker available in large-volume lysed whole blood samples into volumes compatible with *Plasmodium falciparum*-specific RDTs. A systematic investigation of immobilized metal affinity chromatography divalent metal species and solid phase supports established the optimal design parameters necessary to create a flow-through column incorporated into a standard pipette tip. The bidirectional flow inherent to this format maximizes mixing efficiency so that in less than 5 min of sample processing, the test band signal intensity was increased up to a factor of twelve from HRPII concentrations as low as 25 pM. In addition, the limit of detection per sample was decreased by a factor of five when compared to the RDT manufacturer's suggested protocol. Both the development process and commercial viability of this application are explored, serving as a potential model for future applications. Published by AIP Publishing. [<http://dx.doi.org/10.1063/1.4984788>]

I. INTRODUCTION

Malaria remains endemic in 97 countries, and the World Health Organization (WHO) estimates that 3.2 billion people are at risk for the disease.¹ Thanks to the coordinated efforts of numerous international health organizations, the goal of elimination is now within reach. Past malaria control efforts demonstrated that achieving this goal would require a long-term commitment to strategic prevention and case monitoring. This level of vigilance prioritizes the need to identify all individuals infected with the parasite, in particular, the asymptomatic carriers that create transmission reservoirs for the disease.^{2,3} The deployment of point-of-care (POC) diagnostics that achieve single parasite limits of detection is crucial to pinpointing these cases. Ideally, these tests would combine the robust and straightforward nature of rapid diagnostic tests (RDTs) with the accuracy of gold standard laboratory analysis.^{4,5}

When RDTs were first introduced in the early 1980s, they provided a promising resource for POC testing. Unfortunately, these tests remain beleaguered by poor sensitivity and inconsistent quality.⁶ Visual interpretation of RDT results is inherently subjective—especially at low

^{a)}W. S. Bauer and K. A. Richardson contributed equally to this work.

parasitemias.^{7,8} As part of an effort to mitigate RDT technical limitations and deliver a more conclusive diagnosis, Miller and Sikes promoted integration of the sample preparation process into the RDT workflow.⁹ Malarial biomarker purification and enrichment methods have the potential to provide more accurate and objective readings by increasing the test line signal at lower parasitemias, therefore making previously undetectable levels of antigen observable.^{10–13}

The structure of one of the most common malarial biomarkers, *Plasmodium falciparum* histidine-rich protein II (HRPII), lends itself to purification using immobilized metal affinity chromatography (IMAC). Since its inception in 1975, IMAC has become a cornerstone in the field of protein purification because of its ability to capture and purify proteins expressed with high histidine content or labeled with histidine-rich moieties.^{14,15} In its most common form, a divalent nickel ion (Ni^{2+}) is immobilized to a chelating ligand anchored to a solid support. The protein's histidine-rich units bind to the free nickel ion through metal chelation chemistry, thereby removing it from its matrix. To elute the isolated protein for use in downstream applications, the IMAC support is exposed to high concentrations of imidazole, histidine's functional side chain, which outcompetes the captured proteins for the Ni^{2+} coordination site. Considering that approximately 34% of HRPII's amino acid residues are histidine, the malarial biomarker possesses a natural avidity for divalent metal capture methods. This chromatographic method's utility in capturing HRPII has previously been demonstrated through the use of IMAC magnetic beads charged with Ni^{2+} .^{10,11,16}

The current study continues to explore the use of IMAC technology through a practical, inexpensive, and ubiquitous format: the pipette tip. By placing a His-affinity resin bed in the end of a standard plastic pipette tip, the pumping action of the pipette draws the sample back and forth across the IMAC support, capturing HRPII on each pass. Such an application enables field deployment of the microfluidic flow-through format requiring nothing more than a manual pipette. Incorporation of this platform also makes the required sample preparation and processing both easy and intuitive, necessitating only basic instruction. Most importantly, biomarker capture and elution could be accomplished in minutes. With these qualities at the forefront, we have created and optimized a pipette-based IMAC system specifically designed for HRPII enrichment. Progressing from a complete investigation of HRPII's binding affinity to an analysis of the solid support structure, we eventually established the ideal parameters for the IMAC purification and concentration of HRPII. After the completion of the optimization process, we examined the manufacturability of this system by contracting with a company specializing in custom pipette-based columns. The resulting commercial prototype was then evaluated for its utility in improving both the signal intensity and detection limit of malaria RDTs.

II. MATERIALS AND METHODS

A. Materials

Recombinant HRPII was graciously provided by PATH (Seattle, WA). D6 *Plasmodium falciparum* malaria stock was cultured in BSL2 facilities at Vanderbilt University. Cube Biotech PureCube Agarose Beads: Ni-NTA, Zn-NTA, Co-NTA, Cu-NTA, Zn-NTA XL, and Zn-IDA XL (Monheim, Germany); Cube Biotech PureCube 1-Step Batch Mini columns (Monheim, Germany); Affymetrix USB PrepEase Histidine-Tagged High Yield Purification Resin (Santa Clara, CA, USA); Jena Bioscience High Density Zinc Agarose and Low Density Zinc Agarose (Jena, Germany); G-Biosciences Zinc Chelating Resin (Geno Technology, St. Louis, MO); Bio-Rad Chellex-100 Resin (Hercules, CA, USA); Clontech TALON Superflow Metal Affinity Resin (Takara Bio Group, Kusatsu, Shiga, Japan); Bioreclamation IVT CPD Pooled Whole Blood (Hicksville, NY, USA); ThermoScientific Nalgene Rapid Flow 0.2 μm filter, Fisher Scientific Certified ACS-Grade Zinc Sulfate crystals, and Fisher Scientific Nitric Acid TraceMetal Grade (ThermoFisher, Waltham, MA, USA); Certipur Certified Reference Material ICP Multi-Element Standard Solution IV, Glycerol obtained from Sigma-Aldrich, and Ethylenediaminetetraacetic acid from Sigma (Merck KGaA, Darmstadt, Germany); Rainin 250 μl Presterilized Wide Orifice Low Retention tips, Cat # RT-250WSLR (Mettler-Toledo, LLC, Columbus, OH, USA); 28 μm stainless steel mesh, Cat # 85385T116 (McMaster-Carr Supply Company, Elmhurst, IL, USA);

and Paracheck[®] Rapid test device for detecting *P. falciparum* malaria (Ver. 3) (Orchid Biomedical Systems, Goa, India) were used.

B. Methods

1. Analysis of divalent metal-HRP_{II} binding kinetics

An Octet RED96 (ForteBio, CA, USA) was employed to measure the binding kinetics of various divalent metals to HRP_{II} through the use of a technology known as bio-layer interferometry (BLI). Within the parameters of the kinetic assay program, experiments were performed in 96-well plates using eight parallel biosensors manually regenerated with CoCl₂, ZnCl₂, NiCl₂, and CuCl₂. The regeneration process involved soaking manufactured nickel-coordinated nitrilotriacetic acid (Ni-NTA) biosensors in a 10 mM glycine pH 2 solution for 30 min to remove the factory-supplied nickel and then incubating them overnight with the appropriate 10 mM metal ion solution. In order to quantify binding affinity, the freshly charged biosensors were equilibrated in phosphate buffered saline (PBS) for 2 min and then incubated for an additional 5 min to incorporate the octet's standard loading step. The tips were then transferred to wells containing fresh PBS for 1 min to create a baseline before moving them to sample wells for a 10 min association step. These wells contained a 1.56 nM to 100 nM titration of recombinant HRP_{II} biomarker diluted in PBS. Once the HRP_{II} binding was complete, the tips were returned to the PBS baseline wells for a 5 min dissociation step. This process was repeated for each of the four divalent metals used. In each iteration, one of the eight wells was designated 0 nM to serve as a blank. A comprehensive set of binding parameters was developed using a one-to-one global fit binding model.

2. Impact of divalent metal selection on HRP_{II} capture

Four different divalent metal ions were screened using identical nitrilotriacetic acid (NTA) ligands and agarose resin bead matrices. In order to test which metal displayed optimal properties for isolating HRP_{II}, 2.5 μ l of each variety of IMAC agarose resin was loaded into Cube Biotech PureCube 1-Step Batch Mini spin columns and tested against samples of parasitized blood to measure the amount of time needed for maximum binding. Spin columns were prepared with the given amount of resin and washed with two bed volumes of 18 M Ω deionized (DI) water and one bed volume of equilibration buffer (50 mM phosphate buffer at pH 8.0, 300 mM NaCl, and 10 mM imidazole). Each resin was tested in triplicate against identical parasitized lysed whole blood samples. Samples were produced by mixing equal volumes of pooled whole blood with lysis buffer (100 mM phosphate buffer at pH 8.0, 600 mM NaCl, and 2% Triton X-100). Lysed samples were first screened through glass wool packed in a syringe and then through a 0.2 μ m filter to accommodate the specifications of the spin column. After filtering, the blood/lysis solution was spiked with 200 parasites/ μ l using lysed D6 *Plasmodium falciparum* malaria parasite. 100 μ l of prepared blood samples were added to each column and mixed on a vortexer (approx. 2000 rpm) for time increments ranging from 1 to 10 min to allow time for the HRP_{II} protein to bind to the resin. Immediately following the mixing incubation, the columns were centrifuged at 14 000 $\times g$ for 1 min to clear the supernatant which was then retained for analysis. 100 μ l of elution buffer (50 mM phosphate buffer at pH 8.0, 300 mM NaCl, and 500 mM imidazole) was added to each tube, and they were incubated again on the vortexer. All samples were eluted over the course of 2 min regardless of their initial binding time. After mixing, the columns were centrifuged again at the same settings, and the eluent retained for analysis. Prior studies utilizing metal affinity bead binding and elution were used to select initial binding and elution parameters.^{10,11,16} Only one binding time was tested during this phase of the study to serve as a basis for comparison. The concentration of unbound HRP_{II} remaining in the parasitized blood sample and the concentration of HRP_{II} in the eluents were quantified using an HRP_{II} enzyme-linked immunosorbent assay (ELISA).¹¹ The quantification of HRP_{II} in these two samples informs the percentages of HRP_{II} captured and recovered from the original samples for each of the divalent metals as a function of time.

3. Divalent metal loading capacity of commercially available solid phases

Inductively coupled plasma optical emission spectrometry (ICP-OES) was used to compare the amounts of metal loaded on equivalent amounts of resin. 50 μl of each resin were added to identical Cube Biotech spin columns. After washing with DI water to remove all stock solutions, each resin was stripped of its coordinated metal ions using three successive chelation washes of 100 mM EDTA solution, pH 8. The resin columns were incubated on a vortexer for 2 min with 200 μl of 100 mM EDTA solution and then centrifuged for 1 min at $14\,000 \times g$ to collect the supernatant. 100 μl of each chelation wash was diluted in 10 ml of 5% trace metal-free nitric acid solution and quantified using a PerkinElmer Optima 7000 DV ICP-OES standardized using the Certipur multi-element reference solution. The total amount of metal ions chelated in each wash was calculated and compared.

4. Standardization based on divalent metal concentration

All resins were standardized based on their number of zinc metal coordination sites. To determine the number of coordination sites, the factory-loaded metal ions were removed from identical volumes of resin, and then the same resin was recharged with Zn^{2+} ions. In a procedure similar to the one used previously to measure the vendor's loading of divalent metals on each resin, equal amounts of the various resins were loaded into the same spin columns. After two initial washes to remove the stock solution, each resin was subjected to five chelation washes. Each wash consisted of a 5 min incubation on a vortexer with 300 μl of 100 mM EDTA solution, pH 8, followed by a centrifugation at $16\,000 \times g$. All washes were retained for analysis to confirm that all metal ions had been fully stripped. Following the removal of the original metal ions, the resin was washed several times with DI water to ensure the complete removal of EDTA. Once the remaining EDTA had been cleared, each resin column was incubated for 5 min on the vortexer with 300 μl of 100 mM zinc sulfate solution and centrifuged at $16\,000 \times g$. This process was repeated two more times for a total of three regeneration incubations. (As Chellex resin does not come with a metal ion preloaded, it was included in the experiment at the beginning of the regeneration wash steps.) After the resins had been recharged, they were washed again with DI water to remove any residual zinc sulfate solution. At this point, the reloaded resins were stripped again using a chelation process identical to the one used to remove the original metal ions. Upon completion, 100 μl of each chelation wash was diluted in 10 ml of 5% trace metal-free nitric acid solution and analyzed with the same ICP-OES instrument. Final washes were also analyzed to confirm that they were completely free of divalent metal ions. Using these data, the resins were standardized by comparing their individual Zn^{2+} loading capacities to the quantity of Zn^{2+} on the manufactured Cube Biotech PureCube Zn-NTA agarose resin and calculating the amount of resin necessary to achieve the same quantity of Zn^{2+} ions.

5. Solid phase selection

To select the type of resin that would be the most efficient at isolating HRPII, Cube Biotech mini spin columns were each loaded with the volume of resin needed to contain an amount of Zn^{2+} equivalent to that of 5 μl of Cube Biotech PureCube Zn-NTA agarose. Each quantity of resin was stripped and recharged individually using the method previously described. Once each of the resins had been regenerated and washed, a timed binding experiment identical to the procedure employed earlier to examine the binding efficacy of the different metals was conducted to compare the various resins. As the original binding experiment validated the potential for complete capture within 1 min, that time point was the only one tested. The 2 min elution time remained unchanged. Again, ELISA was utilized to quantify the results. The resins exhibiting the highest binding and elution efficiencies were selected to proceed to the next stage.

6. Determine optimal packing of prototype flow-through pipette tips

To determine the optimal resin volume and packing level needed to effectively bind and elute HRPII in the IMAC tip format, varying quantities of resin were loaded into stainless steel mesh fritted tips that were constructed in-house for use with manual Eppendorf Research Plus 20–200 μl pipettes. Each tip was made from two Rainin 250 μl Universal-fit Presterilized Wide Orifice Low Retention tips. Using a 3-D printed cutting guide, the end of each tip was cut off approximately 3 mm from the end to provide a wider surface area for fritting. The end was then pressed directly into a small square of 28 μm stainless steel mesh that had been pre-heated on a hot plate until the tip melted into the frit. After the newly fritted tips had cooled, the excess mesh was trimmed away. The upper frits were made in the same manner except the top of each pipette tip was also cut away so only the last 4 mm attached to the frit remained. Once the modified fritted upper tip was inserted into the top of the fritted bottom tip, each assembled pipette tip contained an approximately 20 μl chamber to hold the resin. See [supplementary material](#) for visual representation (Fig. S1).

Both the Jena Low-Density Zn-IDA and the PrepEase High-Yield resins were recharged with Zn^{2+} in 300 μl batches using the procedure detailed earlier, modified to process larger resin lots in 1.5 ml Eppendorf tubes. The two resins that would be used with the manufacturer's original metal ion loading were added to their own 1.5 ml tubes and included in the final wash steps to ensure a similar preparation with the associated resin loss. After removing the final wash, 300 μl of phosphate buffered saline with 0.1% Tween 20 (PBST) was added to each resin to achieve a 50% (v/v) suspension. The resuspended resins were then pipetted into each tip at resin volumes of 2.5, 5, 10, 15, and 20 μl and prepared in triplicate.

Once the IMAC tip was loaded onto the pipette, fluid was steadily taken in and expelled for the allotted duration of each step. First, 100 μl of equilibration buffer was steadily pumped in and out for 1 min. Immediately after, the tip was transferred to another tube containing 100 μl of parasitized blood/lysis solution prepared using the same method engaged for both binding experiments with only the 0.2 μm filtration omitted. One minute of binding time was allowed for this step, and, again, the supernatant was retained for testing. After completely expelling the sample solution, the tip was transferred to a third tube containing 20 μl of elution buffer. All samples were eluted by pipetting the buffer up and down for a 1 min period. Both the binding supernatants and eluents were quantified using ELISA.

7. Evaluation of elution processing in prototype flow-through pipette tips

In-house fritted pipette tips were also used to examine the conditions needed to maximize HRPII recovery. First, the volume of the elution reagent was measured against the time of elution processing. As both factors determine the residence time of the reagent, it was deemed appropriate to explore both conditions at once. A single Zn^{2+} -charged resin at a fixed amount (10 μl) was selected for this experiment to establish a baseline for comparison. Each sample was processed in a manner similar to the previous experiment. A 1 min equilibration step preceded a 2 min binding step ensured complete capture of the biomarker in a 100 μl lysed blood sample at a parasitemia of 200 parasites/ μl . Four elution times were tested: 15 s, 30 s, 1 min, and 2 min. Each time point was processed with six different volumes of elution reagent ranging from 10 μl to 60 μl to determine which combination would provide the most effective elution parameters.

In conjunction with this experiment, Paracheck RDTs were tested for their tolerance to increased sample volume. Samples were constructed by spiking increasing volumes of elution buffer with a fixed amount of parasite culture to determine how the increased volume would alter test line presentation. Each RDT was processed according to the manufacturer's instructions and analyzed using an ESE Quant Lateral Flow Reader (Qiagen, Germany).

8. Performance validation of commercial 200 μl flow-through columns

Large batches of custom Zn^{2+} -loaded resins were produced using the same method as before then submitted for manufacture into custom column pipette tips based on the optimized

parameters generated in the previous experiments. Photographs of the custom Zn^{2+} flow-through columns are available in the [supplementary material](#) (Fig. S2). Once the tips were acquired, a preliminary test was conducted to ensure that the manufacturer's glycerol-based stabilization fluid would not negatively impact HRPII binding or elution. This was accomplished by filling identical prototype tips containing the equivalent amount of recharged resin with pure glycerol and then processing using established binding and elution times but varying the equilibration time from 1 to 5 min. The volume of equilibration buffer used was also adjusted to 300 μl to provide adequate dilution of the glycerol. As binding and elution appeared unaffected by the addition of the stabilization liquid, the validation moved forward as planned.

First, the 200 μl tips were evaluated using the previously established processing protocol and three elution buffers containing 600, 700, and 800 mM of imidazole. Equilibration time remained at 1 min although the increased equilibration buffer volume was maintained. A full 2 min binding time was used for all samples to ensure complete biomarker collection. The elution step also remained at 30 s irrespective of the variations in imidazole concentration. In order to verify recovery, a second elution step was employed to gauge efficiency. Sample preparation procedures were identical to those used in the previous experiment. Each test was performed in triplicate. HRPII content of binding supernatants and final eluents were analysed using ELISA.

9. Evaluation of 1 mL commercial flow-through columns

The custom manufactured 1000 μl columns tips were evaluated separately. To accommodate the larger tip dimensions, the elution reagent volume was increased to 30 μl as the original amount failed to adequately cover the resin chamber. Otherwise, the equilibration and elution parameters remained the same. In order to fully gauge the advantages afforded by the increased tip volume, samples of 250, 500, 750, and 1000 μl were tested against binding times of 2, 3, and 4 min for each of the resins. Triplicate mock samples were prepared using the same methodology as before, but the parasitemia was reduced to a concentration of 50 parasites/ μl to prevent potential saturation that could skew the results and to provide a more realistic approximation of test samples from asymptomatic patients. Again, the supernatants and eluents were quantified with HRPII ELISA.

10. Evaluation of flow-through columns on the limit of detection of commercially available RDTs

Parasitized blood samples processed using the 200 and 1000 μl tips under the optimized parameters were evaluated using Paracheck RDTs. Whole blood samples were spiked with parasite culture equating to 800 pM HRPII and serially diluted two-fold down to 0.79 pM for use with the 200 μl columns. The 1000 μl columns tested a dilution series ranging from 3.13 pM down to 0 pM. Afterwards, the parasitized whole blood was combined with the lysis solution in a 1:1 ratio and filtered through glass wool to remove cellular debris. 200 μl lysed blood volumes were used for the 200 μl columns and 1000 μl for the 1000 μl columns. The complete titration series was performed in triplicate using each column's optimized protocol with the exception of a final adjustment made to the 1000 μl column elution step. Rather than using the tested elution buffer, 700 mM imidazole was spiked into Paracheck's own running buffer, and the two-drop volume ($\sim 50 \mu\text{l}$) was cycled through the column. The results from pre-processed samples were compared with the results from Paracheck RDTs performed according to the manufacturer's approved protocol using the same blood specimen lots. Each RDT was scanned and quantitated using the ESEQuant Lateral Flow Reader. These readings were used to generate "Area under the curve" measurements for test line signals in this concentration range for both flow-through column processed samples and control samples.

III. RESULTS AND DISCUSSION

A. Quantitative binding kinetics and equilibration of divalent metal-HRPII interaction

Ni(II)NTA is commonly used to purify recombinant proteins expressed with six consecutive histidine (hexahis) residues because of its high affinity and selectivity for this tag under

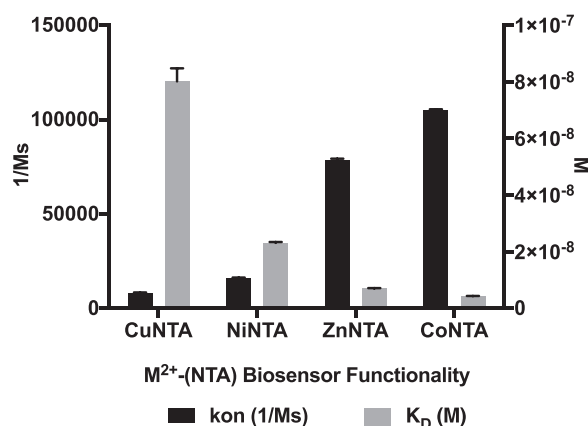


FIG. 1. Molecular binding characterization of divalent metals with HRPII. Kinetic (black columns) and equilibrium (grey columns) binding data between Cu(II), Ni(II), Zn(II), and Co(II)-NTA data generated employing BLI. We explore how a balance of these characteristics may result in the most desirable outcome.

relatively mild conditions. The Ni(II)NTA system has been utilized to capture and concentrate HRPII, but to date, no systematic investigation has been conducted into the use of other divalent metals and chelating ligands.^{10,11} Although affinity-specificity correlations have been drawn between IMAC metal coordination chemistry and histidine-rich moieties, we have found no reports of quantitative kinetic data on the interaction between divalent metals and HRPII. Through the employment of BLI, a powerful label-free technique that measures biomolecular interactions in direct binding assays, a comprehensive set of equilibrium and kinetic data for HRPII binding was generated for each of the four divalent metals that commonly participate in IMAC metal coordination chemistry (Fig. 1). The results reflect the general affinity and specificity trends reported for the hexahis-M⁺-NTA system.⁹ To validate the regeneration protocol and ensure that the data obtained were a product of the divalent metal interaction with HRPII rather than a consequence of biosensor manipulation, manufactured Ni(II)NTA biosensors were compared to biosensors that had been stripped and recharged with divalent nickel. No significant difference was observed (Fig. S3, [supplementary material](#)).

When selecting a divalent metal to rapidly capture HRPII and elute under mild conditions, kinetic and equilibrium tradeoffs must be considered. A large association constant (k_{on}) represents the metal that facilitates the fastest capture, while a small equilibration constant (K_D) promotes a tight binding interaction to achieve strong retention. However, the opposite characteristics are desirable when trying to accomplish fast and effective elution. Ideally, a balance between kinetic attributes is the most desirable model to attain reversible capture. According to the BLI results, divalent zinc and cobalt best fit this character. At $7.5 \times 10^4 \text{ M}^{-1} \text{ s}^{-1}$, Zn^{2+} has the second highest k_{on} just below Co^{2+} 's at $1.1 \times 10^5 \text{ M}^{-1} \text{ s}^{-1}$. Divalent Nickel generated a K_{on} of $1.6 \times 10^4 \text{ M}^{-1} \text{ s}^{-1}$ and Cu^{2+} generated the lowest K_{on} value at $8.2 \times 10^3 \text{ M}^{-1} \text{ s}^{-1}$. Divalent zinc and cobalt also exhibited the lowest K_D 's at $9.0 \times 10^{-9} \text{ M}$ and $5.0 \times 10^{-9} \text{ M}$, respectively (Fig. 1). Divalent Nickel displayed a K_D of $2.3 \times 10^{-8} \text{ M}$ and Cu^{2+} had the poorest K_D at $8.0 \times 10^{-8} \text{ M}$.

B. Divalent metal-HRPII binding utilizing a model agarose solid phase

Cube Biotech resin was selected for use as a model solid phase to explore the active binding kinetics of the same four common coordinating divalent metals with HRPII. To investigate how the different metal species participate in the capture and elution of HRPII in a complex matrix, the four different metal-loaded versions of this resin were evaluated by their ability to bind and elute HRPII as a function of time from parasitized lysed whole blood samples. In parallel, sister aliquots of the same resins were analyzed for the total divalent metal content. This molar quantity signifies the total number of binding sites involved in the capture and elution of HRPII. By generating ratios of HRPII bound and HRPII released to the total amount of divalent

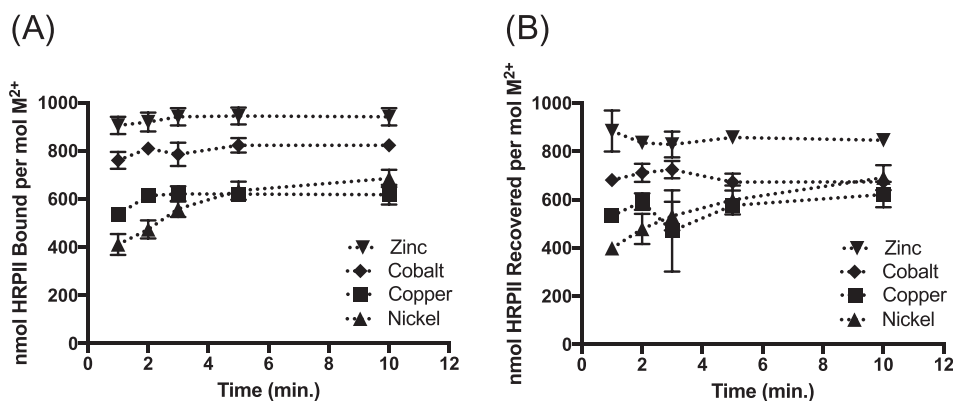


FIG. 2. Impact of divalent metal selection on HRP II binding and recovery. HRP II binding (a) and recovery (b) performance of each divalent metal based on total HRP II binding per mol of divalent metal anchored to the solid phase. In both capacities, Zn^{2+} -loaded resins outperformed the other metals tested. Note: Error bars may be obscured by the data point icon.

metal per sample, performance metrics of nmols HRP II per mole of divalent metal were determined for each activity (Fig. 2).

These results clearly identify zinc as the optimal divalent metal for HRP II capture and recovery. It presents a key balance of kinetic characteristics, allowing it to quickly bind HRP II yet not so tightly as to inhibit elution. The data also reveal that the most commonly used metal in IMAC chemistry, Ni^{2+} , actually performs quite poorly regarding HRP II capture within a complex matrix. Its poor binding and elution behavior add minutes to the total processing time and lead to incomplete recovery. Substituting zinc for nickel has the potential to substantially improve the performance of IMAC chemistry in HRP II applications.

C. Solid phase selection for flow-through device

There are a number of different solid support materials available encompassing a variety of features including structural material, support monodispersity, functionalization location (surface, internal, mixed), chelate ligand, thermal tolerance, and storage stability. To determine the optimal characteristics needed for the proposed system, eight different commercially available resins representing a variety of these features were selected and screened for HRP II binding and recovery efficiencies. A table with complete descriptions of all IMAC solid phases tested in this study can be found in the [supplementary material](#) (Table S1).

While Zn^{2+} was found to be the most desirable divalent metal to employ in an HRP II extraction device, its performance could be enhanced or impeded by the qualities of the solid support. To quantify this effect on the binding and recovery of HRP II, each of the eight IMAC solid phases included in the screen was functionalized with Zn^{2+} . First, a reference metal loading density was determined for each of the candidate resins through the stripping and quantification of the factory-loaded metals [Fig. 3(a)]. After regeneration with divalent zinc, the resins were stripped again, and the Zn^{2+} loading was quantitated and compared to the original amount. [Fig. 3(b)]. The recharging protocol was optimized to ensure that all divalent metal ions were removed from each solid phase (Figs. S4 and S5, [supplementary material](#)). Even if the commercially available resin was originally functionalized with Zn^{2+} , it underwent regeneration to ensure that all IMAC resins were subject to identical treatments. As a general trend, the loading density of the factory metal was less than that of the regeneration. With the Zn^{2+} loading density determined, a measure based on the number of divalent metal atoms per unit volume of regenerated IMAC resin was produced. This measurement allowed all resins to be standardized with the same total number of Zn^{2+} binding sites. This normalization afforded an independent investigation of solid phase performance in HRP II capture [Fig. 3(c)] and elution [Fig. 3(d)].

These data show that although five different types of Zn^{2+} -functionalized resins exhibit capture higher than 90%, only CubeBiotech Zn-NTA, Jena Low Density Zn-IDA, and PrepEase

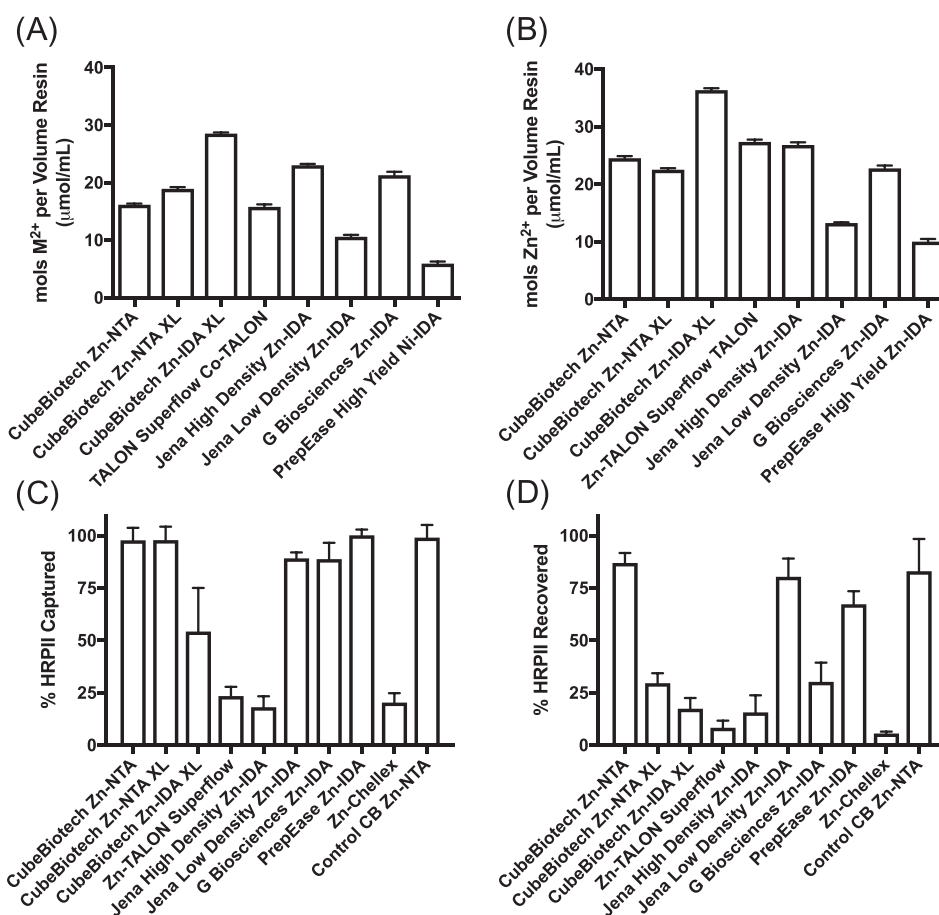


FIG. 3. IMAC solid phase characterization and performance screen. Factory divalent metal loading density for each resin (a) with their corresponding Zn^{2+} loading densities (b) following the Zn^{2+} metal regeneration protocol provided a basis for normalization to fixed number of Zn^{2+} binding sites. The Zn^{2+} -normalized resins were evaluated using fixed binding and elution times for the capture (c) and recovery (d) of the total molecules of HRP II.

Zn-IDA can efficiently elute more than 80% of the captured HRP II. In general, there was no correlation between the characteristics exhibited by the different solid phases and their subsequent performance in this screen. All three were synthesized with different chelating ligands and varied in terms of size, material, and monodispersity (Table S1, [supplementary material](#)). One noticeable trend found in this study was that resins with lower Zn^{2+} loading densities exhibited increased elution. This observation suggests that a higher density of Zn^{2+} may facilitate the rebinding of HRP II to neighboring coordination sites during elution, decreasing the overall elution efficiency. CubeBiotech Zn-NTA exhibited more moderate Zn^{2+} loading levels yet maintained strong elution behavior. From this difference, it could also be inferred that overall performance is determined by the combined effects of metal loading, ligand, and support. As with the kinetics findings, it appears that a balance of characteristics is necessary for optimal results.

D. Development of a prototype flow-through device with general processing parameters

The three best performing resins, CubeBiotech Zn-NTA, Jena Low Density Zn-IDA, and PrepEase Zn-IDA, were chosen as the preferred resins for flow-through pipette tip column development. To discover optimal design parameters for HRP II capture and elution, in-house fritted column tips were constructed as prototypes. Optimal resin loading was determined by pipetting parasite-spiked, lysed whole blood through a range of packed bed volumes and measuring the amount of HRP II extracted. Fully packed resin beds appeared to lack the interstitial space necessary for the viscous lysed whole blood solution to pass through given the pipette's

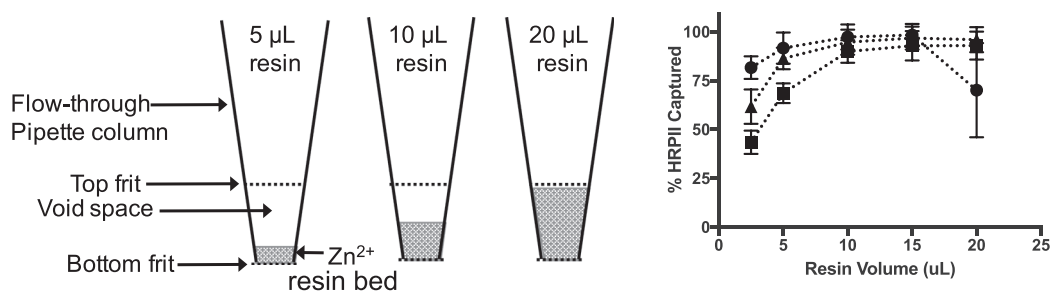


FIG. 4. Evaluating packed bed resin for HRP2 capture performance. As described in the above diagram, various resin volumes were packed into pipette columns constructed in-house. These volumes were tested against Cube Biotech Zn(II)NTA (circles), PrepEase Zn(II)IDA (triangles), and Jena low density Zn(II)IDA (squares) resins to evaluate HRP2 capture efficiency in a lysed whole blood matrix.

limited vacuum generation. In contrast, loosely packed columns provided more mixing of the solid and mobile phases but lacked the total surface area and residence time needed to completely capture HRP2 within the cycle. 10 µL resin beds, or columns half-filled with resin, produced the optimal balance of movement and contact without risk of clogging. HRP2 capture efficiencies of 97.7 ± 6.45 , 94.7 ± 6.4 , and $90.0 \pm 5.75\%$ were observed for CubeBiotech Zn-NTA, PrepEase Zn-IDA, and Jena Low Density Zn-IDA, respectively (Fig. 4).

In order to optimize HRP2 elution from a flow-through device, the in-house fritted pipette tips were packed at the optimal 50% level with 10 µL of a single resin [Cube Biotech Zn(II)NTA]. To examine the impact of elution reagent volume and processing time on the retrieval of HRP2, this experiment juxtaposed different traverse cycling time points against different elution volumes to discover which combination produced the most effective recovery. A 30 s elution time proved optimal at all reagent volumes tested with the 20 µL volume providing the highest release at $78.0 \pm 19.1\%$ of the bound protein [Fig. 5(a)]. The recovery decrease associated with increased elution times is likely the result of two primary factors: HRP2 rebinding to the solid phase during the longer residence and cycling-induced aeration hindering contact with the elution reagent.

The elution volume of the proposed flow-through system also has implications in the function of the commercial RDTs. As shown in Fig. 5(b), a fixed amount of HRP2 dissolved in increasing volumes of elution reagent produces a decrease in the test line signal when tests are otherwise performed according to the manufacturer's protocol. This phenomenon is likely the result of drastically reducing HRP2's residence time in the conjugate pad. Substantially increasing the test volume with a fluid much less viscous than blood increases its mobility in relation to the gold signal reporter, abbreviating the binding window. To avoid this effect, the smallest volume that can efficiently elute the captured HRP2 from the flow-through column should be used so as not to lose signal.

The last elution parameter tested was the concentration of the competitive liberating agent, imidazole. The percentage of captured HRP2 eluted was monitored as a function of increasing imidazole concentration. By employing the optimal elution parameters of a 20 µL reagent volume and a 30 s cycling time, a peak concentration range of imidazole was identified between 600 and 800 mM [Fig. 5(c)].

E. Evaluation of a manufactured Zn²⁺ flow-through device

Following the initial optimization of the capture and elution of HRP2 using a prototype flow-through column, the three prospective Zn²⁺-regenerated resins identified in the solid phase selection, PrepEase (VUP), Jena Low Density (VUJ), and Cube Biotech (VUC), were prepared and delivered to a commercial manufacturer to be constructed into a flow-through column based on our design parameters. The manufacturer loaded the selected resins into both 200 µL and 1000 µL pipette tips using their patented method, which also included the addition of a proprietary glycerol-based liquid to each column, aiding in the stabilization of hydrated resin tips at

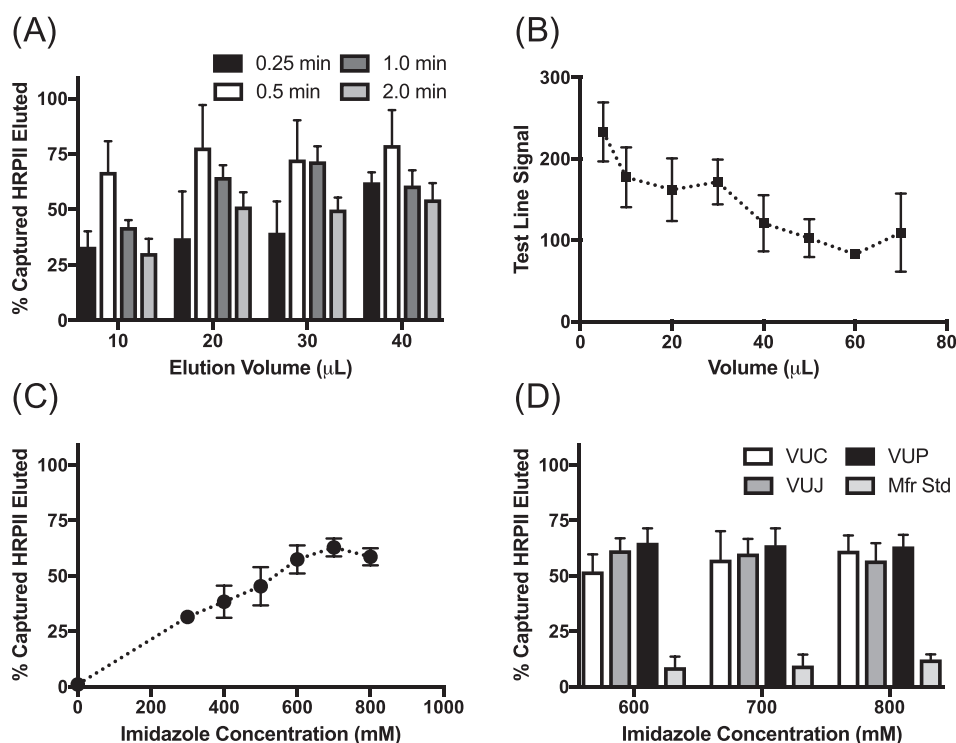


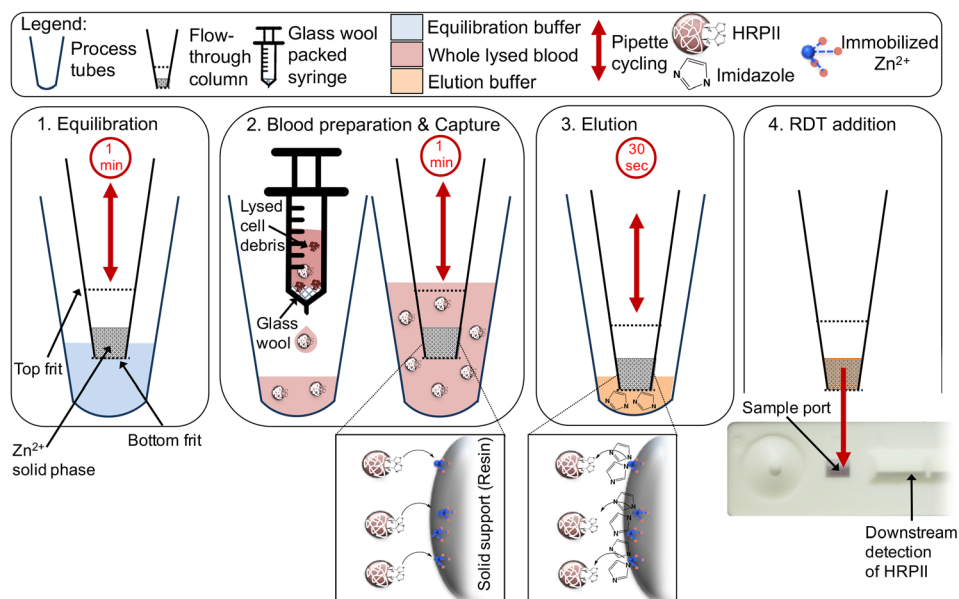
FIG. 5. Optimizing the elution parameters for Zn^{2+} flow-through columns. (a) Evaluation of the % of captured HRPII eluted from the column as a function of elution volume and pipette cycling time. (b) The effects of increased elution volume on RDT signal. (c) Optimization of imidazole elution concentration for the prototype columns. (d) Final imidazole optimization of the manufactured Zn^{2+} flow-through columns.

room temperature. The manufacturer's own Ni-IMAC His binding columns were also procured in order to compare the experimental columns to a known commercial standard.

The purpose of this process was to explore the translation of our laboratory-developed sample preparation column into a commercially manufactured format. Both columns possessed approximately the same size fritted resin chambers and were subsequently packed with the same amount of bed resin (10 μ l). The 200 μ l manufactured flow-through columns were validated using the processing times and reagent volumes previously determined using the in-house prototype. In addition to the overall device validation, this study also included a more focused evaluation of the elution reagent's imidazole concentration, further assessing the three peak values ranging from 600 to 800 mM. As no significant difference in HRPII elution was observed, the 700 mM imidazole median concentration was selected for use in the remaining experiments [Fig. 5(d)].

Of the three resins validated using 700 mM elution buffer, the VUP candidate yielding $61.8\% \pm 7.1\%$ capture of the total HRPII available in the 200 μ l whole lysed blood samples was selected to demonstrate the device's capacity to increase the visual intensity of RDT test lines. The decrease in HRPII recovery appears to be the result of a confluence of factors which will be addressed more fully in the Technical Notes section. The completely optimized 3 min process is visualized in Scheme 1. The 1000 μ l pipette columns were examined in terms of their capture efficiency in handling increasing sample volumes over extended processing times. The overall capture and elution efficiencies for 1000 μ l tips containing VUP were similar, and of the binding times tested, the 3 min cycle was deemed sufficient regardless of volume (Figs. S6 and S7, [supplementary material](#)).

The RDT enhancement step was evaluated using an ESEQuant Lateral Flow Reader. Employment of the RDT reader provided an objective quantification of the test line signal, directly comparing the enriched samples to the 5 μ l whole blood control RDTs. The native antigen concentrations used in the parasitized lysed blood samples ranged from 0.8 pM (46.6 pg/ml) to 800 pM (47.2 ng/ml) HRPII (Fig. 6). The biomarker concentration region between 0 and



SCHEME 1. Operation principle for flow-through pipette column. (1) First, the pipette column is subjected to an equilibration step where the stabilization formula is expelled from the column and the column is hydrated by pipetting and depressing the pipette in 300 μ l of equilibration buffer for 1 min, or approximately 4 pipette traverse cycles. (2) Following the equilibration step, the column is introduced to a glass wool-filtered whole lysed blood sample where it is once again cycled for 1 min to enable HRP II capture. (3) It then is transferred to a final preparation tube where it cycles 20 μ l of 700 mM imidazole elution buffer for 30 s before (4) all eluent is ejected from the tip directly onto the RDT for downstream detection of HRP II.

50 pM HRP II is often difficult to interpret since faint, poorly developed test lines can be missed by health workers possessing reduced visual acuity or those operating in reduced lighting conditions.¹⁷ Taking the ratio of “area under the curve” values of the enhanced samples by that of the control yields an average signal improvement of 6.8-fold at each of the antigen concentrations within this region. The most pronounced enhancement was observed at 25 pM HRP II with a 12.6-fold augmentation. These results demonstrate that pre-processing with a flow-through column increases RDT test line intensity and enables signal saturation at lower antigen concentrations per sample when compared to controls. This outcome will improve interpretation of test lines and promote more accurate diagnoses by healthcare workers.

A unique advantage of this preparation strategy lies in its ability to increase an RDT’s standard limit of detection. The flow-through format easily adapts to larger pre-processed blood volumes, allowing more biomarker to be captured, concentrated, and delivered to the RDTs. This

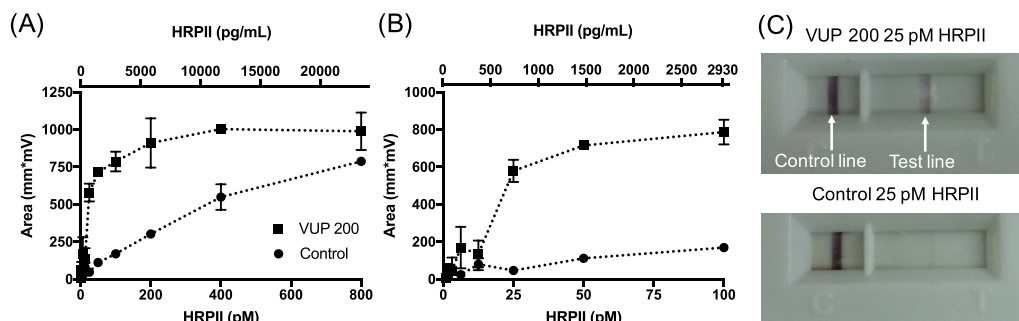


FIG. 6. Increased LFA signal employing flow-through column process. (a) Reflectance signal measurements from RDTs processed with VUP 200 (squares) flow-through columns and control manufacturer suggested protocol (circles). (b) A detail of the 0–100 pM HRP II concentration regime and (c) representative RDTs for VUP 200 processed (top) and control (bottom) RDTs at 25 pM HRP II. An average enhancement of 6.8-fold was achieved for the 0–50 pM region.

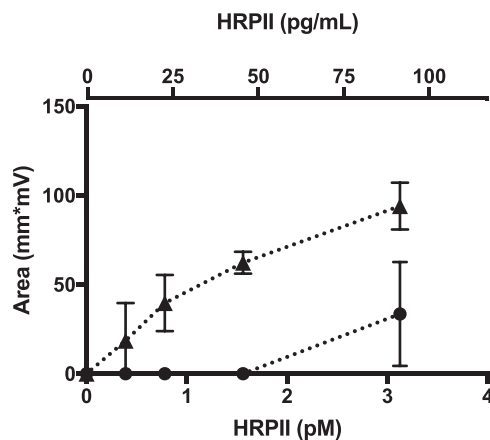


FIG. 7. Detection limit increase. Reflectance signal measurements from RDTs processed with VUP 1000 (triangles) flow-through columns and control 5 μ l additions according to the manufacturer suggested protocol (circles). The detection limit was lowered to 0.78 pM or approximately 0.35 p/ μ l.

benefit enables visual detection of extremely low antigen concentrations, which might otherwise go undetected. The approach used to determine detection limit used in this study aligns with the WHO-FIND method for evaluating commercial RDTs.¹ Samples were processed in triplicate, and the lowest antigen concentration that yielded three consecutive positive RDTs was determined to be the detection limit. The RDT reader was set at signal threshold of 15 mm²mV, where reflectance readings that were less than the threshold would not register a positive reading. This threshold limit was selected because of its correlation with the visual limit of detection as determined by the researchers in this study. The Paracheck-Pf RDT was chosen as an evaluation tool, because it ranks as one of the top performing commercial RDTs.¹ Using this established methodology, the Paracheck RDT achieves a detection limit of 3.13 pM HRPII under the manufacturer's intended protocol.

To explore the utility of the flow-through column as a means to increase detection limits, the RDT's established limit of detection was compared to the enhanced detection limit found using the 1 ml pipette column format (labeled as 1000 VUP) with 500 μ l whole blood samples containing 0–3.13 pM (185 pg/ml) HRPII (Fig. 7). A 500 μ l whole blood sample represents the maximum practical sample volume that can be acquired through finger stick according to the Centers for Disease Control and Prevention.¹⁸ The end result suggests that while this RDT attains a 3.13 pM HRPII limit of detection per the intended protocol, the VUP 1000 flow-through column enhancement decreased this detection limit to 0.78 pM HRPII. In addition, two of three 0.39 pM samples tested yielded positive RDT readings. Although the relationship between the HRPII concentration and parasite density is life-stage dependent, the correlation found for the parasite stock culture used in this study suggests that 0.78 pM HRPII is the equivalent of approximately 0.35 parasites/ μ l.

F. Technical notes

Although the use of a pipette based flow-through column shows great potential as a front-end RDT sample preparation strategy, we identified some technical limitations during its development. First, lysed whole blood tends to clog the porous frit in this format necessitating the use of a glass-wool filtration step to remove the larger cellular debris. While lysing whole blood is necessary to ensure that all HRPII biomarker is available for capture, this unintended side effect could be mitigated through an increase in the frit's pore size, allowing the debris to traverse unimpeded. The VUP resin that was ultimately selected in this study possesses an average diameter of $\sim 90 \mu$ m, a size that allows for a substantial increase from the 24 μ m filter mesh used by the manufacturer.

Another notable issue discovered during the elution step was that the movement of the small volumes of liquid through the solid phase induced bubbling and aeration that diminished

HRPII recovery and inhibited effective transfer of eluent to the RDT. Larger volumes of reagent tended to alleviate this issue, but the RDT's failure to successfully incorporate significant increases in sample volume precluded a complete exploration of this as an option. The culmination of these effects became even more pronounced in the 1 ml tips as adequate contact between the elution buffer and resin became more difficult given the increased interstitial space. Incorporation of the manufacturer's own running buffer into the elution step provided a substantial volume increase partially mitigating this outcome.

G. Discussion

The World Health Assembly's Global Technical Strategy for Malaria articulates goals of a 90% reduction in malaria infections as well as elimination in 35 new countries.¹⁹ While large gains can be made through simple resource allocation, full elimination requires targeted efforts such as Mass Screen and Treat (MST) programs.²⁰ Implementation of such initiatives becomes even more challenging when faced with the isolated and rural areas common in malaria-endemic regions. This scarcity of health care facilities and trained personnel has led to an increase in the procurement and use of malaria RDTs, and although more than 80 commercial RDTs are currently available, their low sensitivity and subjective interpretation often hinder the efficacy of these malaria-control programs.^{20,21}

The most common mistake made by novice test users is misinterpreting a faint positive or invalid RDT as negative.²² The intensity of the test line is dependent on antigen levels but varies with matrix factors including blood viscosity and blood volume.^{23,24} Matrix-induced anomalies such as incomplete clearing and red background make it more difficult to interpret these tests. These specific anomalies are found in 95% and 85% of products, respectively.²⁵ Integration of a brief, user-friendly sample preparation strategy into RDT procedures is the most straightforward solution for removing anomalies associated with the blood matrix and increasing the intensity of test lines at lower HRPII concentrations. However, there are no generally accepted sample preparation strategies for RDTs. Our group has previously developed several magnetic bead-based HRPII extraction approaches that employ metal affinity magnetic beads to capture and escort HRPII to RDTs.^{10,11,16} The key advantages of these systems include resistance to micro-channel clogging and direct elution of the magnetic capture beads deposited onto the RDT. This direct deposition of the solid phase onto the RDT promotes more effective HRPII elution and improved limits of detections. However, this system is hampered by longer processing times, more user steps, battery-powered equipment, and higher cost. In contrast, the pipette-based system described in this paper has shorter processing time, needs fewer user steps, requires less equipment, and is less expensive. Although this system does not reach the sensitivity of the magnetic bead-based system, we did achieve a limit of detection suitable for the identification of asymptomatic patients (0.35 parasites/ μ l) with a method more suited to low resource settings. A recent model generated by Slater *et al.* estimates that this threshold will detect greater than 95% of the infectious disease reservoir.²⁶

A more practical advantage of the pipette-based flow-through column is its potential for manufacture and commercialization. A commonly unaddressed aspect of POC diagnostic development is cost. This is often a critical barrier that ultimately determines the future of these technologies. While the prototype columns used in this study averaged \$2.08 per unit, the economies of scale in conjunction with the growing number of manufacturers offering pipette tip modification will serve to drive down cost. Unlike other technologies requiring the development of manufacturing platforms, full commercialization of this format could be achieved in the short term through collaboration with an industry partner. The established stability of silica-based resin ensures that this technology will remain field deployable, obviating the need for cold-chain storage and indicating a longer shelf life.²⁷

Additional avenues that merit exploration are the use of other materials for the capture of HRPII. Such options include paper monoliths formed with capillary valves or functionalized nitrocellulose.^{28,29} These materials can conceivably optimize antigen delivery to RDTs impacting their performance. Another direction we would like to pursue involves the modification of

the pipette requirement, either by incorporation of the flow-through column into a disposable unit or through development of a modular component that can produce the cycling vacuum needed to process each tip. All of these technologies present opportunities to further customize this form factor to increase both its efficiency and deployability.

Constructing this processing platform using proven tools and techniques further establishes the robustness of the design concept. Adapting familiar applications to this specific purpose will also serve to overcome the resistance associated with the adoption of new technologies. Together, this combination of factors supports its capacity for commercialization. The possibilities associated with this low-cost, easy-to-use platform are not limited to HRPII; other antigens found in complex matrices could also be purified and enriched for detection by RDT or through other labeled or label-free strategies.

IV. CONCLUSION

In this study, we established the potential of a flow-through pipette column as a clinical tool to increase the performance of current POC diagnostic technologies. Through extensive characterization and testing, we demonstrated how native HRPII could be concentrated from larger patient samples and then released for downstream detection. While this sample pre-processing strategy was used to enhance the sensitivity of a single brand of lateral flow RDTs, we elucidate a method that can easily be adapted to other *Plasmodium falciparum* diagnostics targeting HRPII such as bench-top enzyme-linked immunosorbent assays (ELISA) or other spectroscopic methods where larger elution volumes do not hinder signal output.^{22–24} Full development and deployment of this device offer a means for improving on existing diagnostic technologies to further malaria elimination efforts.

SUPPLEMENTARY MATERIAL

See [supplementary material](#) for descriptions of the prototype flow-through column construction, validation figures for the divalent metal regeneration protocol, relevant physical properties for the different IMAC solid phases used in this study, and figures summarizing the 1 ml VUP flow-through column optimization.

ACKNOWLEDGMENTS

The authors would like to thank Dr. Kim Fong for culturing D6 *Plasmodium falciparum* used in this work, Austin Hardcastle for prototype production assistance, and M. F. Richards for critical comments concerning the manuscript. We would like to acknowledge Vanderbilt University for support from the Laboratories for Innovations in Global Health Technologies (LIGHT). We acknowledge funding from Intellectual Ventures/Global Good (Bellevue, WA).

¹World Health Organization, *Malaria Rapid Diagnostic Test Performance: Results of WHO Product Testing of Malaria RDTs: Round 6 (2014–2015)* (WHO, 2015).

²L. Wu, L. L. van den Hoogen, H. Slater, P. G. T. Walker, A. C. Ghani, C. J. Drakeley, and L. C. Okell, “Comparison of diagnostics for the detection of asymptomatic *Plasmodium falciparum* infections to inform control and elimination strategies,” *Nature* **528**, S86–S93 (2015).

³M. L. McMorro, M. Aidoo, and S. P. Kachur, “Malaria rapid diagnostic tests in elimination settings—can they find the last parasite?,” *Clin. Microbiol. Infect.* **17**(11), 1624–1631 (2011).

⁴P. Yager, G. J. Domingo, and J. Gerdes, “Point-of-care diagnostics for global health,” *Annu. Rev. Biomed. Eng.* **10**, 107–144 (2008).

⁵P. B. Lippa, C. Müller, A. Schlichtiger, and H. Schlebusch, “Point-of-care testing (POCT): Current techniques and future perspectives,” *Trends Anal. Chem.* **30**(6), 887–898 (2011).

⁶S. Sharma, J. Zapatero-Rodríguez, P. Estrela, and R. O’Kennedy, “Point-of-care diagnostics in low resource settings: present status and future role of microfluidics,” *Biosensors* **5**, 577–601 (2015).

⁷P. Mukadi, P. Gillet, B. Barbe, J. Luamba, A. Lukuka, J. Likwela, D. Mumba, J. J. Muyembe, P. Lutumba, and J. Jacobs, “SMS photograph-based external quality assessment of reading and interpretation of malaria rapid diagnostic tests in the Democratic Republic of the Congo,” *Malaria J.* **14**, 26 (2015).

⁸T. F. Scherr, S. Gupta, D. W. Wright, and F. R. Haselton, “Mobile phone imaging and cloud-based analysis for standardized malaria detection and reporting,” *Sci. Rep. – Uk.* **6**, 28645 (2016).

⁹E. Miller and H. D. Sikes, “Addressing barriers to the development and adoption of rapid diagnostic tests in global health,” *Nanobiomedicine* **2**, 6 (2015).

- ¹⁰K. M. Davis, L. E. Gibson, F. R. Haselton, and D. W. Wright, "Simple sample processing enhances malaria rapid diagnostic test performance," *Analyst* **139**(12), 3026–3031 (2014).
- ¹¹K. M. Davis, J. D. Swartz, F. R. Haselton, and D. W. Wright, "Low-resource method for extracting the malarial biomarker histidine-rich protein II to enhance diagnostic test performance," *Anal. Chem.* **84**(14), 6136–6142 (2012).
- ¹²M. A. Nash, J. N. Waitumbi, A. S. Hoffman, P. Yager, and P. S. Stayton, "Multiplexed enrichment and detection of malarial biomarkers using a stimuli-responsive iron oxide and gold nanoparticle reagent system," *ACS Nano* **6**(8), 6776–6785 (2012).
- ¹³G. A. Posthuma-Trumpie, J. Korf, and A. van Amerongen, "Lateral flow (immuno)assay: Its strengths, weaknesses, opportunities and threats: A literature survey," *Anal. Bioanal. Chem.* **393**, 569–582 (2009).
- ¹⁴J. Porath, J. Carlsson, I. Olsson, and G. Belfrage, "Metal chelate affinity chromatography, a new approach to protein fractionation," *Nature* **258**(5536), 598–599 (1975).
- ¹⁵H. Block, B. Maertens, A. Spriestersbach, N. Brinker, J. Kubicek, R. Fabis, J. Labahn, and F. Schafer, "Immobilized-metal affinity chromatography (IMAC): A review," *Method Enzymol.* **463**, 439–473 (2009).
- ¹⁶K. M. Ricks, N. M. Adams, T. F. Scherr, F. R. Haselton, and D. W. Wright, "Direct transfer of HRP-II-magnetic bead complexes to malaria rapid diagnostic tests significantly improves test sensitivity," *Malaria J.* **15**(1), 399 (2016).
- ¹⁷M. L. Gatton, R. R. Rees-Channer, J. Glenn, J. W. Barnwell, Q. Cheng, P. L. Chiodini, S. Incardona, I. J. Gonzalez, and J. Cunningham, "Pan-Plasmodium band sensitivity for Plasmodium falciparum detection in combination malaria rapid diagnostic tests and implications for clinical management," *Malaria J.* **14**, 115 (2015).
- ¹⁸Centers for Disease Control and Prevention, see https://www.cdc.gov/labstandards/pdf/vitaleqa/Poster_Capillary_Blood.pdf for Steps for Collecting Finger Stick Capillary Blood Using a Microtainer.
- ¹⁹World Health Organization, *Global Technical Strategy for Malaria 2016–2030* (WHO, United Kingdom, 2016).
- ²⁰A. B. Tiono, A. Ouedraogo, A. Diarra, S. Coulibaly, I. Soulama, A. T. Konate, A. Barry, A. Mukhopadhyay, S. B. Sirima, and K. Hamed, "Lessons learned from the use of HRP-2 based rapid diagnostic test in community-wide screening and treatment of asymptomatic carriers of Plasmodium falciparum in Burkina Faso," *Malaria J.* **13**, 30 (2014).
- ²¹World Health Organization, List of Known Commercially-Available Antigen-Detecting Malaria RDTs, see [http://www.wpro.who.int/malaria/internet/resources.ashx/RDT/docs/MD_table34%2B\(1\)_totalistofISO131485criteria.pdf](http://www.wpro.who.int/malaria/internet/resources.ashx/RDT/docs/MD_table34%2B(1)_totalistofISO131485criteria.pdf) for Information for national public health services and UN Agencies wishing to procure RDTs (last accessed May 14, 2017).
- ²²S. A. Harvey, L. Jennings, M. Chinyama, F. Masaninga, K. Mulholland, and D. R. Bell, "Improving community health worker use of malaria rapid diagnostic tests in Zambia: Package instructions, job aid and job aid-plus-training," *Malaria J.* **7**, 160 (2008).
- ²³World Health Organization, *Malaria Rapid Diagnosis, Making it Work, Informal Consultation on Field Trials and Quality Assurance on Malaria Rapid Diagnostic Tests, 20–23 January 2003 Report* (WHO Regional Office for the Western Pacific Manila, 2003).
- ²⁴R. W. Peeling, P. G. Smith, and P. M. M. Bossuyt, "A guide for diagnostic evaluations," *Nat. Rev. Microbiol.* **4**(Suppl.), S2–S6 (2010).
- ²⁵World Health Organization, *Malaria Rapid Diagnostic Test Performance: Results of WHO Product Testing of Malaria RDTs: Rounds 1–6 (2008–2015)* (WHO, 2015).
- ²⁶H. C. Slater, A. Ross, A. L. Ouedraogo, L. J. White, C. Nguon, P. G. T. Walker, P. Ngor, R. Aguas, S. P. Silal, A. M. Dondorp, P. La Barre, R. Burton, R. W. Sauerwein, C. Drakeley, T. A. Smith, T. Bousema, and A. C. Ghani, "Assessing the impact of next-generation rapid diagnostic tests on Plasmodium falciparum malaria elimination strategies," *Nature* **528**(7580), S94–S101 (2015).
- ²⁷R. Stock and C. B. F. Rice, *Chromatographic Methods* (Springer, 2013), p. 74.
- ²⁸P. Floris, D. Connolly, B. White, and A. Morrin, "Development and characterisation of switchable polyaniline-functionalised flow-through capillary monoliths," *RSC Adv.* **4**(83), 43934–43941 (2014).
- ²⁹C. A. Holstein, A. Chevalier, S. Bennett, C. E. Anderson, K. Keniston, C. Olsen, B. Li, B. Bales, D. R. Moore, E. Fu, D. Baker, and P. Yager, "Immobilizing affinity proteins to nitrocellulose: a toolbox for paper-based assay developers," *Anal. Bioanal. Chem.* **408**(5), 1335–1346 (2016).